NATIONAL ADVISORY COMMITTEE FOR AERONAUTICS

REPORT No. 854

COMPRESSIBILITY EFFECTS ON THE LONGITUDINAL STABILITY AND CONTROL OF A PURSUIT-TYPE AIRPLANE AS MEASURED IN FLIGHT

By WILLIAM N. TURNER, PAUL J. STEFFEN
and LAWRENCE A. CLOUSING

1946

For sale by the Superintendent of Documents, U. S. Government Printing Office, Washington 25, D. C. - - - - - - - - - - - Price 15 cents

AERONAUTIC SYMBOLS

1. FUNDAMENTAL AND DERIVED UNITS

	Symbol	Metric		English	
		Unit	Abbreviation	Unit	Abbreviation
Length	l	meter	m	foot (or mile)	ft (or mi)
Time	t	second	s	second (or hour)	sec (or hr)
Force	F	weight of 1 kilogram	kg	weight of 1 pound	lb
Power	P	horsepower (metric)		horsepower	hp
Speed	V	kilometers per hour	kph	miles per hour	mph
		meters per second	mps	feet per second	fps

2. GENERAL SYMBOLS

W Weight $=mg$

g Standard acceleration of gravity $=9.80665$ m/s^2 or 32.1740 ft/sec^2

m Mass $=\frac{W}{g}$

I Moment of inertia $=mk^2$. (Indicate axis of radius of gyration k by proper subscript.)

μ Coefficient of viscosity

ν Kinematic viscosity

ρ Density (mass per unit volume)

Standard density of dry air, 0.12497 kg-m^{-4}-s^2 at 15° C and 760 mm; or 0.002378 lb-ft^{-4} sec^2

Specific weight of "standard" air, 1.2255 kg/m^3 or 0.07651 lb/cu ft

3. AERODYNAMIC SYMBOLS

S Area

S_w Area of wing

G Gap

b Span

c Chord

A Aspect ratio, $\frac{b^2}{S}$

V True air speed

q Dynamic pressure, $\frac{1}{2}\rho V^2$

L Lift, absolute coefficient $C_L=\frac{L}{qS}$

D Drag, absolute coefficient $C_D=\frac{D}{qS}$

D_0 Profile drag, absolute coefficient $C_{D_0}=\frac{D_0}{qS}$

D_i Induced drag, absolute coefficient $C_{D_i}=\frac{D_i}{qS}$

D_p Parasite drag, absolute coefficient $C_{D_p}=\frac{D_p}{qS}$

C Cross-wind force, absolute coefficient $C_C=\frac{C}{qS}$

i_w Angle of setting of wings (relative to thrust line)

i_t Angle of stabilizer setting (relative to thrust line)

Q Resultant moment

Ω Resultant angular velocity

R Reynolds number, $\rho\frac{Vl}{\mu}$ where l is a linear dimension (e.g., for an airfoil of 1.0 ft chord, 100 mph, standard pressure at 15° C, the corresponding Reynolds number is 935,400; or for an airfoil of 1.0 m chord, 100 mps, the corresponding Reynolds number is 6,865,000)

α Angle of attack

ϵ Angle of downwash

α_0 Angle of attack, infinite aspect ratio

α_i Angle of attack, induced

α_a Angle of attack, absolute (measured from zero-lift position)

γ Flight-path angle

REPORT No. 854

COMPRESSIBILITY EFFECTS ON THE LONGITUDINAL STABILITY AND CONTROL OF A PURSUIT-TYPE AIRPLANE AS MEASURED IN FLIGHT

By WILLIAM N. TURNER, PAUL J. STEFFEN
and LAWRENCE A. CLOUSING

Ames Aeronautical Laboratory
Moffett Field, Calif.

National Advisory Committee for Aeronautics

Headquarters, 1500 New Hampshire Avenue NW, Washington 25, D. C.

Created by act of Congress approved March 3, 1915, for the supervision and direction of the scientific study of the problems of flight (U. S. Code, title 49, sec. 241). Its membership was increased to 15 by act approved March 2, 1929. The members are appointed by the President, and serve as such without compensation.

TECHNICAL COMMITTEES

AERODYANMICS
POWER PLANTS FOR AIRCRAFT
AIRCRAFT CONSTRUCTION
OPERATING PROBLEMS
MATERIALS RESEARCH COORDINATION
SELF-PROPELLED GUIDED MISSILES
SURPLUS AIRCRAFT RESEARCH
INDUSTRY CONSULTING COMMITTEE

Coordination of Research Needs of Military and Civil Aviation
Preparation of Research Programs
Allocation of Problems
Prevention of Duplication
Consideration of Inventions

LANGLEY MEMORIAL AERONAUTICAL LABORATORY, Langley Field, Va.

AMES AERONAUTICAL LABORATORY, Moffett Field, Calif.

AIRCRAFT ENGINE RESEARCH LABORATORY, Cleveland Airport, Cleveland, Ohio

Conduct, under unified control, for all agencies, of scientific research on the fundamental problems of flight

---

OFFICE OF AERONAUTICAL INTELLIGENCE, Washington, D. C.

Collection, classification, compilation, and dissemination of scientific and technical information on aeronautics

REPORT No. 854

COMPRESSIBILITY EFFECTS ON THE LONGITUDINAL STABILITY AND CONTROL OF A PURSUIT-TYPE AIRPLANE AS MEASURED IN FLIGHT

By William N. Turner, Paul J. Steffen, and Lawrence A. Clousing

SUMMARY

Measurements of the longitudinal stability and control of a pursuit-type airplane were made in flight up to a Mach number of 0.78. The data are presented in the form of curves showing the variation, with center-of-gravity position, dynamic pressure, and Mach number, of the stick-fixed and stick-free stability, control, and balance of the airplane.

It was found that large increases in stability occurred at high Mach numbers, reducing the controllability of the airplane. Large increases in diving moment were also encountered at high Mach numbers and moderate lift coefficients. These changes were caused almost entirely by increases in the tail angle of attack and the rate of change of tail angle of attack with airplane lift coefficient resulting from the shock-stalling of the wing. An increment of stalling moment, however, was encountered at high Mach numbers and very low lift coefficients, apparently caused by a negative shift in the airplane angle of zero lift.

Distortion of the elevator fabric at high speeds, but not necessarily high Mach numbers, caused the stick-free neutral point as measured in steady straight flight to move far rearward and increased the stick-force gradient in accelerated flight.

INTRODUCTION

For the past several years the National Advisory Committee for Aeronautics has been conducting an extensive flight program for the purpose of obtaining quantitative design criterions to insure favorable handling qualities of airplanes. Practically all of these data, however, have been obtained at speeds below those at which the compressibility of the air appreciably affects the characteristics of the airplane. The capability of modern aircraft to reach high Mach numbers has made essential further investigations of the critical changes that occur in the stability and control characteristics due to compressibility. Because of the hazards involved in investigating unfamiliar regions in flight, most of the present knowledge of this subject has been obtained in wind-tunnel tests of airfoil sections and airplane models. Although the tunnel results have been of great value in indicating the problems that would be encountered and the methods of solution, complete appreciation of the effects actually encountered in flight must finally be obtained from flight tests of actual aircraft.

The purpose of the present investigation was to provide information on the longitudinal stability and control characteristics of a typical conventional pursuit airplane, to determine not only what happened to the airplane but also why it happened, to substantiate the pertinent general effects of the compressibility phenomena as indicated in the wind tunnel, and to provide data for aid in further evaluating and developing the flying-qualities specifications.

The data were obtained from static-stability flight tests conducted at four center-of-gravity positions up to a Mach number of 0.55 and maneuvering-stability tests conducted with the center of gravity at 0.288 M. A. C. up to a Mach number of 0.78. In order to obtain data at the highest Mach numbers, the airplane was flown several times up to the maximum attainable Mach number (about 0.80) by diving vertically from the absolute ceiling (about 34,000 feet), regaining level flight at 12,000 feet.

It is believed that the present investigation is the most comprehensive of its type to date and may indicate general trends to be expected; even so, it only provides a part of the information necessary for a complete general analysis of the problem which, of course, requires tests on many aircraft.

The investigation was made by the NACA at the Ames Aeronautical Laboratory, Moffett Field, Calif.

The symbols used throughout this report are defined in appendix A.

DESCRIPTION OF THE AIRPLANE

The airplane utilized in this investigation was a single-engine, single-place, low-wing, cantilever monoplane equipped with partial-span split flaps and tricycle retractable landing gear.

Pertinent dimensions of the airplane are given in appendix B. Figures 1 and 2 are photographs of the airplane as instrumented for flight tests, and figure 3 is a three-view drawing of the airplane.

INSTRUMENTATION

Standard NACA photographically recording instruments were used to measure, as a function of time, indicated airspeed, pressure altitude, normal acceleration, elevator angle, elevator control force, pitching velocity, manifold pressure, engine speed, propeller-blade angle, and internal pressure in the elevator.

A free-swiveling airspeed head was mounted on a boom about 4 feet ahead of the leading edge of the right wing at

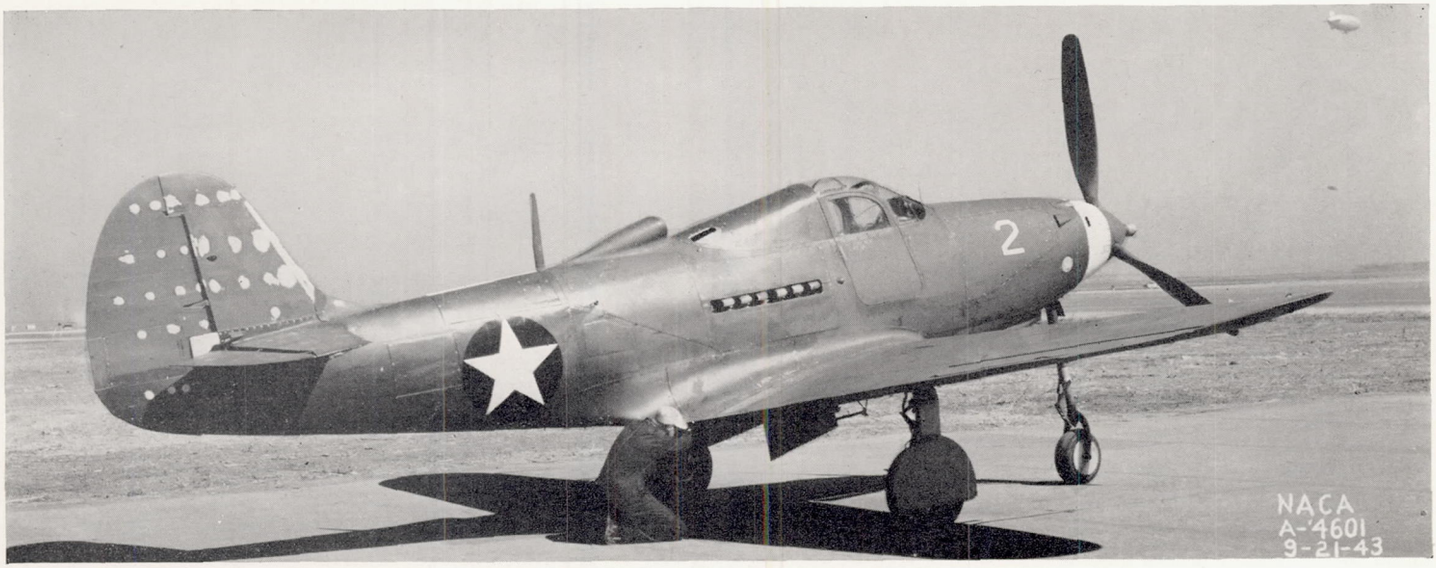

FIGURE 1.—Three-quarter rear view, test airplane.

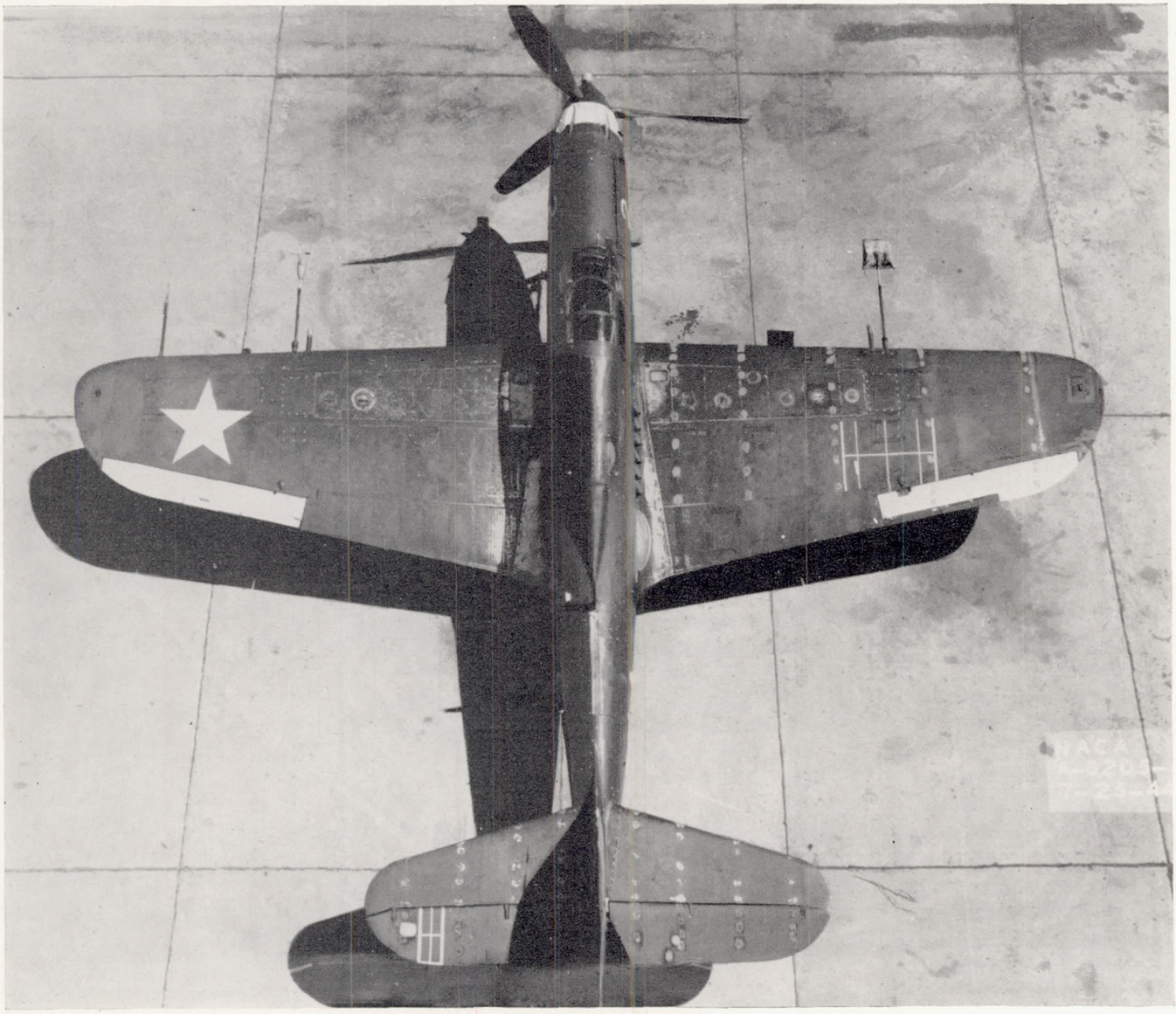

FIGURE 2.—Top view, test airplane as instrumented for flight tests.

a spanwise station about 7 feet inboard from the wing tip. The head consisted of two separate static-pressure tubes (for separate connections to the airspeed recorder and altitude recorder) with a single total-pressure tube between them. The airspeed and altitude recorders were mounted in the wing at the base of the boom. Calibration indicated that the lag in this system was negligible. (See reference 1.)

The static pressure was calibrated for position error by comparing the reading of the recording altimeter with the known pressure altitude as the airplane was flown at several speeds past a reference height. It was assumed that the total pressure was measured correctly. Calibration in the Ames 16-foot wind tunnel showed that the error in recorded airspeed due to the difference in the blocking of the head itself between the highest Mach number obtained in the flight calibration (0.50) and the highest Mach number obtained in these flight tests (0.78) was less than 1 percent.

Indicated airspeed was computed according to the formula by which standard airspeed meters are graduated (gives true airspeed at standard sea-level conditions). The formula may be written as follows:

$$V_i = 1703\left[\left(\frac{H-p}{p_0}+1\right)^{0.286}-1\right]^{1/2}$$

All elevator angles were corrected for stretch in the elevator control system between the elevator and the control-position recorder.

In order to investigate distortion of the fabric, photographs of the upper and lower surfaces of the left elevator were taken with 16-millimeter gun-sight-aiming-point cameras mounted in the base of the fin just above the horizontal tail and in the fuselage just below the horizontal tail. Straight lines painted on the fabric above ribs and between ribs furnished suitable references for evaluating the distortion. (See figs. 2 and 4.) Three additional ribs in which pressure orifices were mounted were installed in each elevator. Their location may be noted in figure 4. The orifices were used in connection with a separate investigation.

TEST PROCEDURE AND CONDITIONS

Data were obtained with four center-of-gravity positions in steady straight flight at Mach numbers [1] below 0.55. This group of data is referred to as "the lower Mach number data."

Further tests were run at Mach numbers from 0.33 to 0.78 with the center of gravity at one location, 0.288 M. A. C. These tests consisted principally of gradual turns or pull-outs. Only the portions of the maneuvers where the pitching acceleration was negligible were used in the data reduction This group of data is referred to as "the higher Mach number data." It was believed that the additional information to be gained from tests with more than one center-of-gravity position at high Mach numbers was not important enough to warrant further risk to the airplane and pilot.

All tests were conducted with flaps and gear up; the oil and coolant shutters were set one-half open (flush with the main fuselage contours). Power-off tests were run with the engine fully throttled and the propeller in the high-pitch

[1] The general relationship between indicated airspeed, pressure altitude, and Mach number is shown in fig. 5.

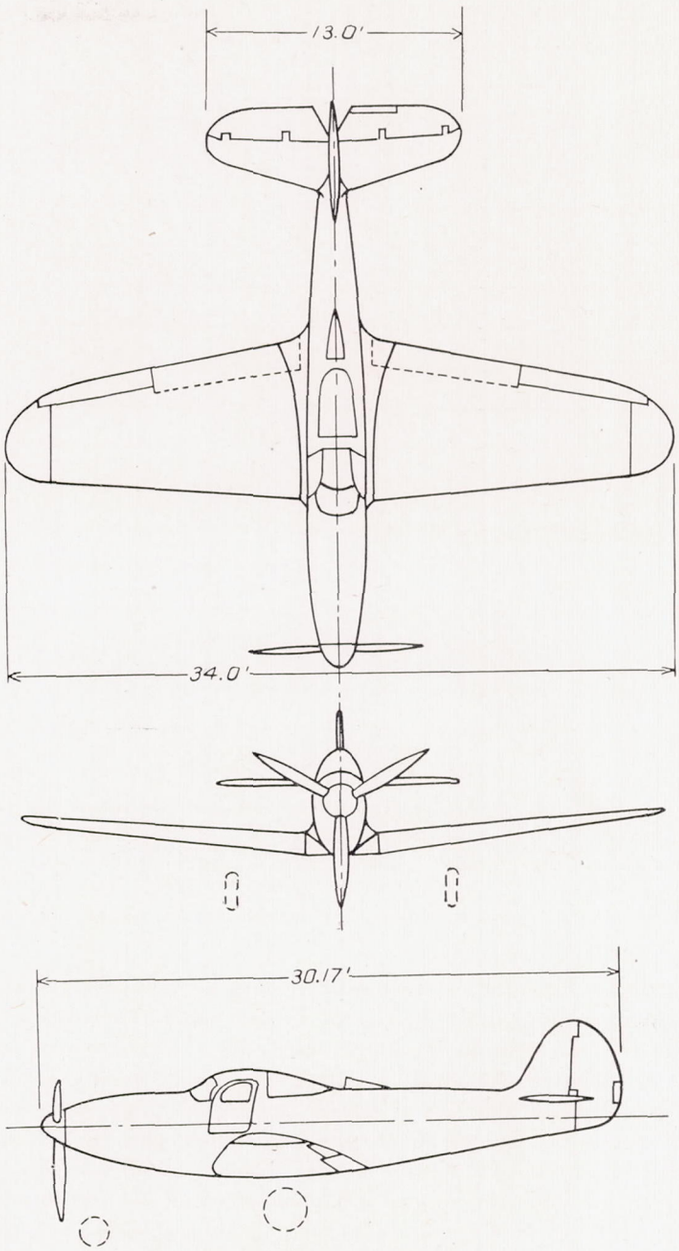

FIGURE 3.—Three-view drawing of the test airplane.

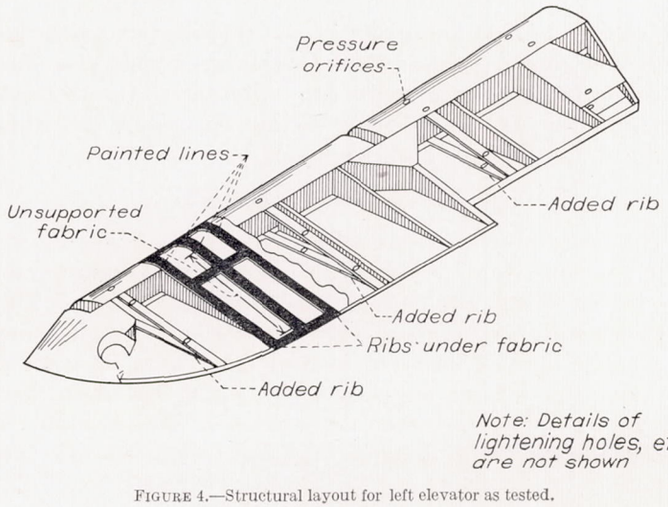

FIGURE 4.—Structural layout for left elevator as tested.

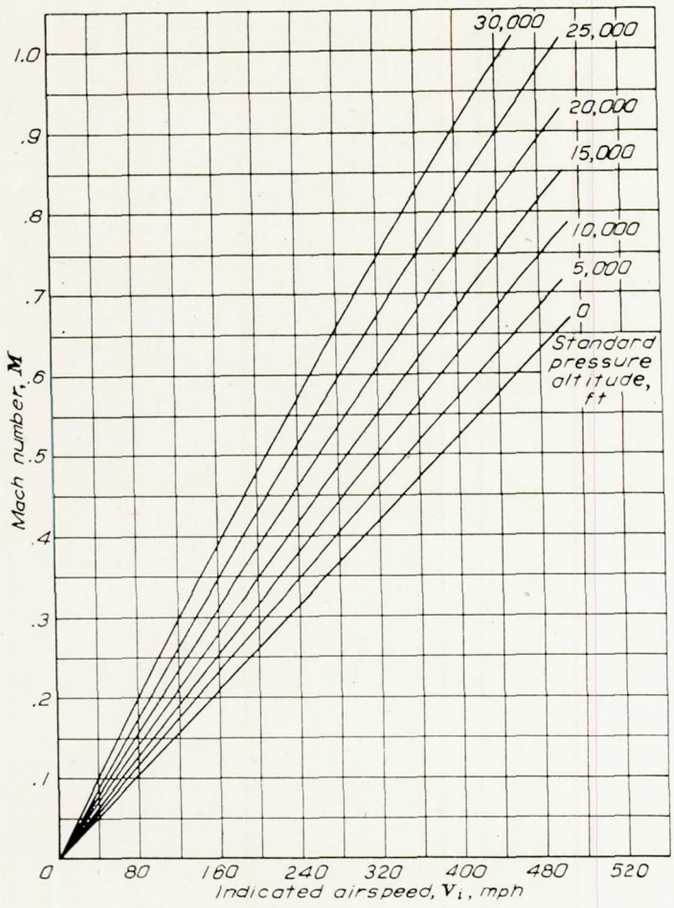

FIGURE 5.—General relationship between indicated airspeed, pressure, altitude, and Mach number.

setting. Power-on tests were run with normal rated power (power settings of 39 in. Hg M. P. and 2,600 r. p. m.) up to the critical altitude; at higher altitudes the power was set at full throttle with 3,000 r. p. m. In some of the dives from high altitude the latter power control settings were not changed even though the airplane was dived past the critical altitude. Curves of the actual values of engine speed, propeller-blade angle, and brake horsepower (as determined by reference to the engine-power charts) resulting from the power settings are shown in figure 6.

PRESENTATION OF THE DATA

So that a unified impression of the organization and scope of the data may be obtained, the curves are briefly described in the order of their presentation. Details of the methods and formulas used in deriving certain curves are described in the section Results and Discussion.

THE LOWER MACH NUMBER DATA

The lower Mach number stick-fixed longitudinal-stability data for the clean configuration are shown in figure 7 for the power-off and the normal-rated-power conditions. This figure includes the basic curves of elevator angle as a function of C_L, the derived curve of neutral point as a function of C_L, and the several cross plots by which the data were faired and the neutral point determined. The variations of Mach number and dynamic pressure with C_L also are indicated.

Similar data showing the stick-free longitudinal stability are presented in figure 8.

The elevator internal-pressure coefficient is shown as a function of elevator angle in figure 9.

Profiles of a typical elevator section between ribs showing the fabric distortion encountered under several flight conditions are presented in figure 10. The profile at the ribs did not become measurably distorted.

The lower Mach number data are compared in appendix C with data obtained on a similar airplane at Langley Memorial Aeronautical Laboratory.

THE HIGHER MACH NUMBER DATA

The measured and derived data obtained from the tests at higher Mach numbers are shown in figures 11 to 17. Although tests were made with both power on and power off at altitudes from 5,000 to 30,000 feet, differences due to changes in power and altitude were not large enough to be separable; the data, therefore, were considered as one group.

Figure 11 shows typical basic stability data (elevator angle and stick-force modulus F_e/q as a function of lift coefficient). Straight lines were used to fair the data; curvatures which apparently were indicated in some instances by the trend of the test points were believed due more to small variations in the Mach number during the high-speed pull-outs than to actual changes in stability with lift coefficient. The faired data in figure 11, along with a large amount of similar data not presented, were cross-plotted and again faired, resulting in the curves of elevator angle as a function of Mach number shown in figure 12 and stick-force modulus as a function of

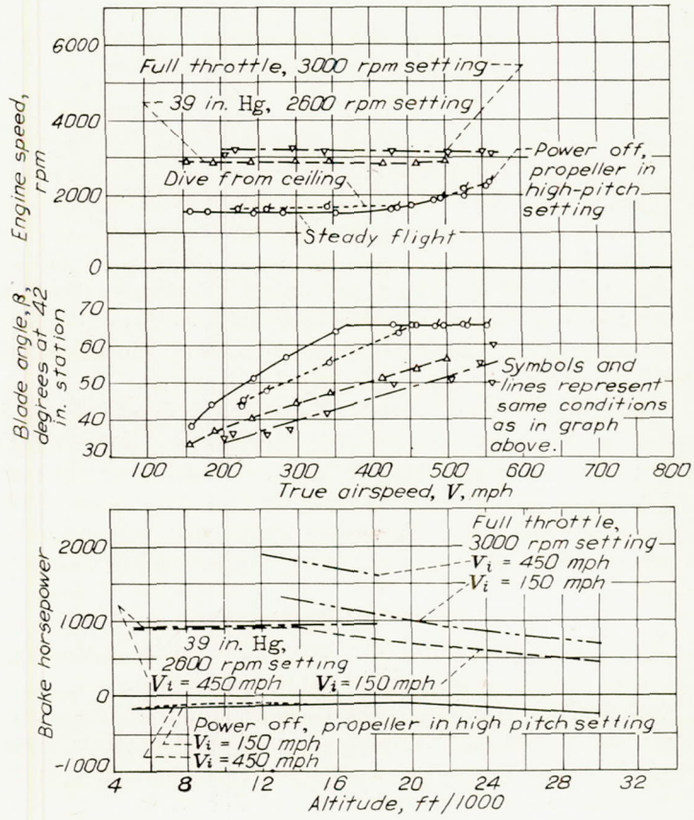

FIGURE 6.—Engine speed, propeller blade angle, and brake horsepower obtained for certain power settings.

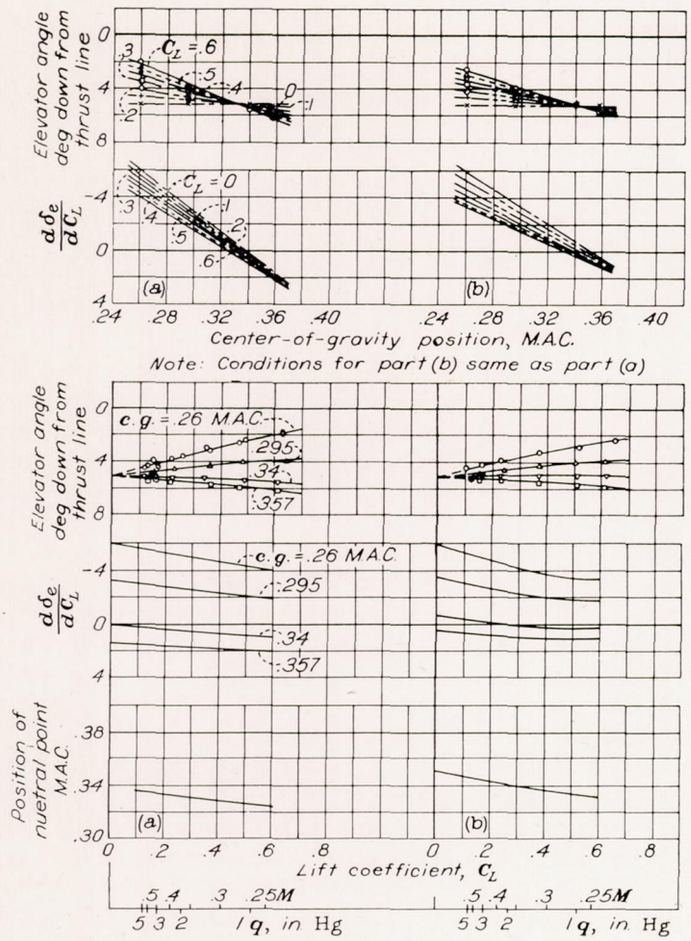

FIGURE 7.—Stick-fixed longitudinal stability characteristics at the lower Mach numbers; clean condition, elevator tab 0.5° down, oil and coolant shutters ½ open, altitude 3,500 to 12,000 feet. (a) Power off, propeller in high-pitch setting. (b) Normal rated power, engine speed 2,600 revolutions per minute.

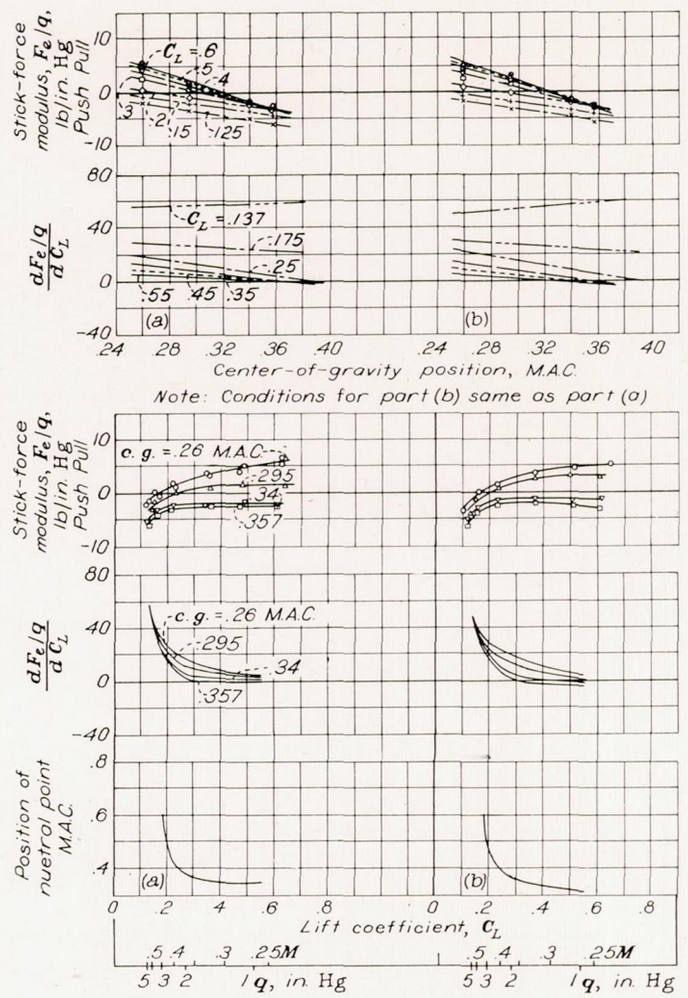

FIGURE 8.—Stick-free longitudinal stability characteristics at the lower Mach numbers; clean condition, elevator tab 0.5° down, oil and coolant shutters ½ open, altitude 3,500 to 12,000 feet. (a) Power off, propeller in high-pitch setting. (b) Normal rated power, engine speed 2,600 revolutions per minute.

Mach number shown in figure 13. The points are included on these figures to indicate the magnitudes of the dispersion in the data. The curves of figures 12 and 13 have been replotted to a common zero axis and cross-plotted as a function of lift coefficient in figures 14 and 15 to indicate more clearly the stability changes involved. Figure 15 also includes curves of F_e/q computed on the assumption that the low-speed hinge-moment coefficients did not vary with Mach number or fabric distortion, thereby enabling the magnitude of these effects to be more readily appreciated.

The data in figures 14 and 15 were used to obtain the stick-fixed and stick-free stability parameters $d\delta_e/dC_L$ and $d(F_e/q)/dC_L$) and tbe neutral point. These parameters are shown in figure 16 as a function of Mach number. The curves of figure 16 with other data then were used to compute the variation of $C_{h_{\delta_e}}$ with Mach number shown in figure 17.

ADDITIONAL DERIVED DATA

The variation with Mach number of the pitching-moment coefficient (about the 0.288 M. A. C. point) of the wing only and of the airplane minus the horizontal tail was computed from the wing pressure-distribution data of reference 2 and from tail pressure-distribution data. The variation is shown

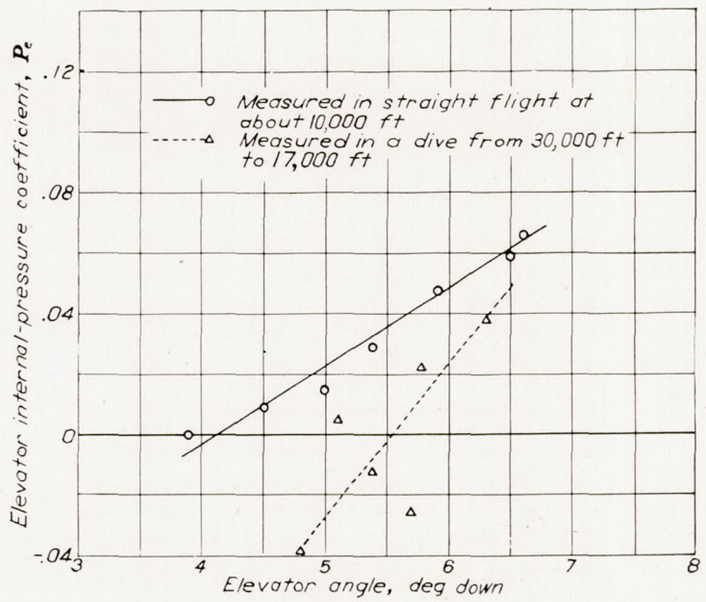

FIGURE 9.—Internal pressure in the elevator.

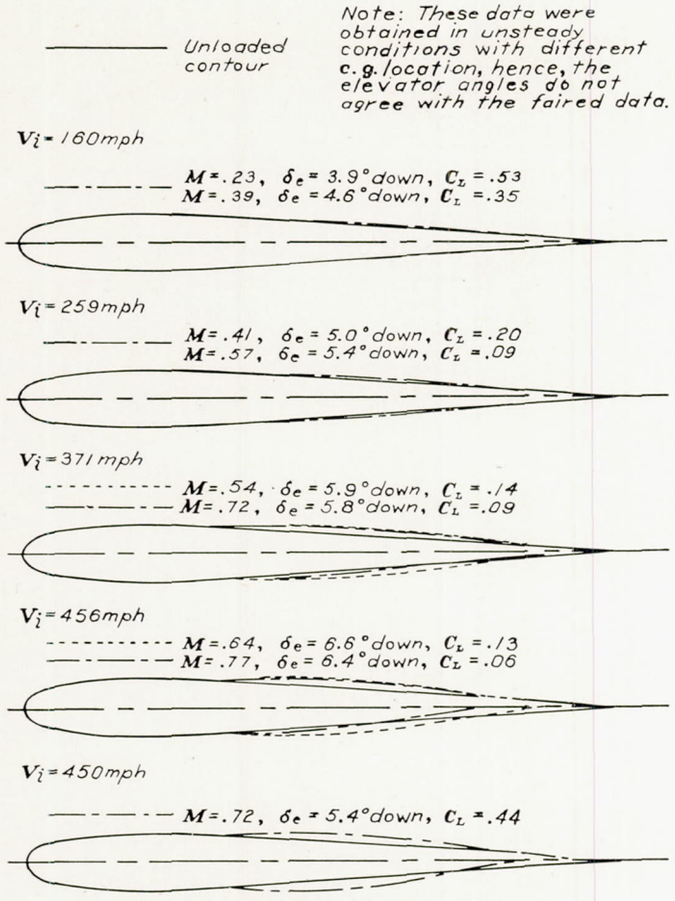

FIGURE 10.—Bulging of the elevator fabric.

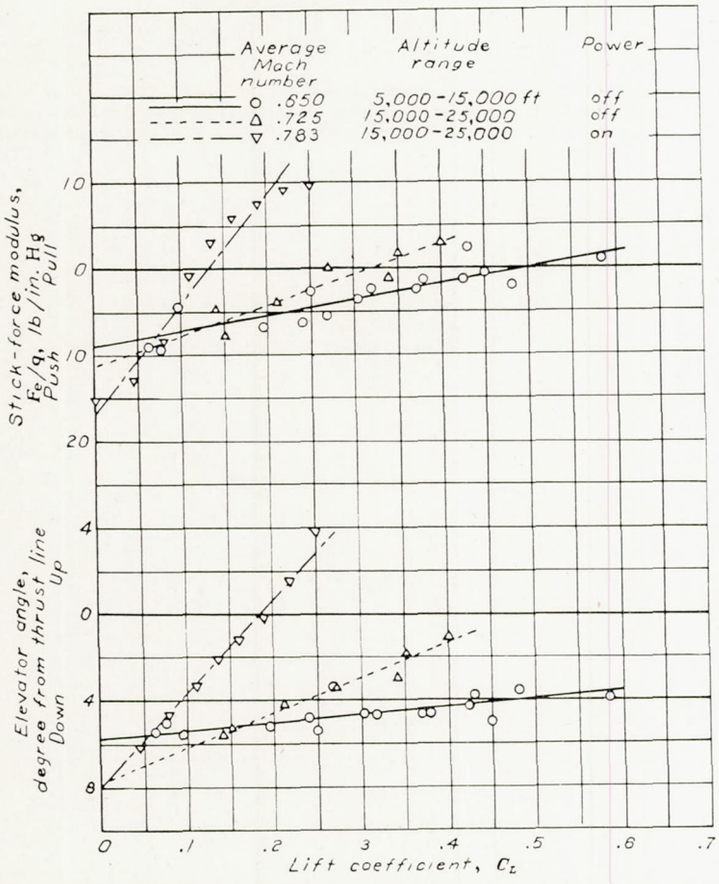

FIGURE 11.—Typical maneuvering-stability data taken at high Mach numbers; clean condition, tab neutral, center of gravity at 0.288 M. A. C.

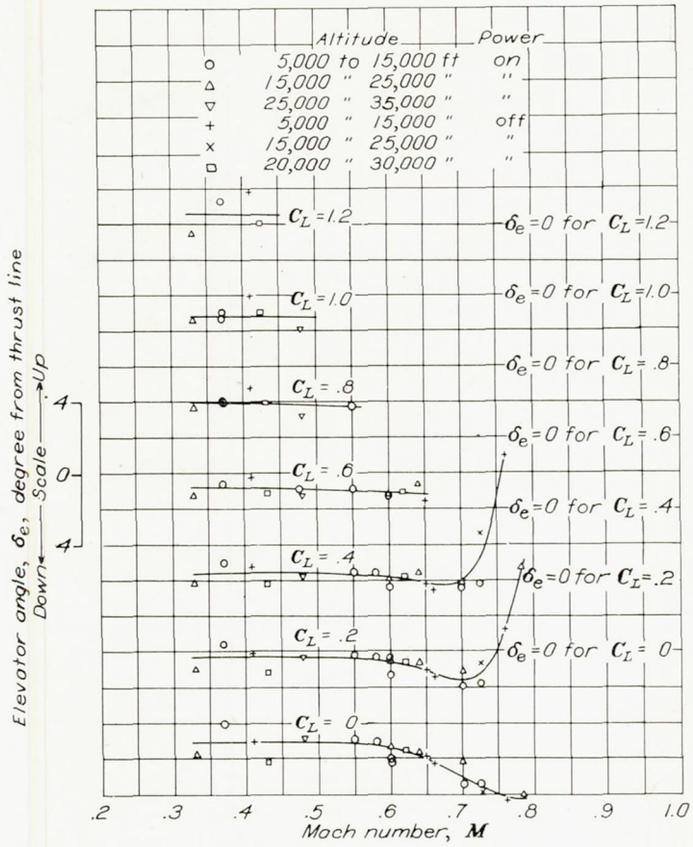

FIGURE 12.—Variation of elevator angle with Mach number; clean condition, tab neutral, c. g. at 0.288 M. A. C. Points are cross-plotted from faired data of figure 11 and similar curves to show the dispersion of the data.

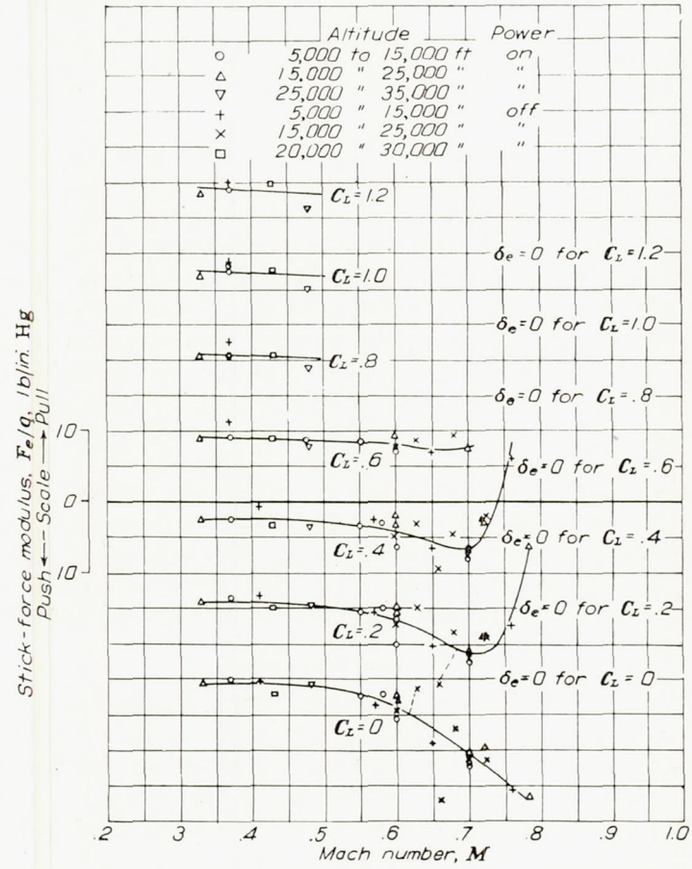

FIGURE 13.—Variation of stick-force modulus with Mach number; clean condition, tab neutral, c. g. at 0.288 M. A. C. Points are cross-plotted from faired data of figure 11 and similar curves to show the dispersion of the data.

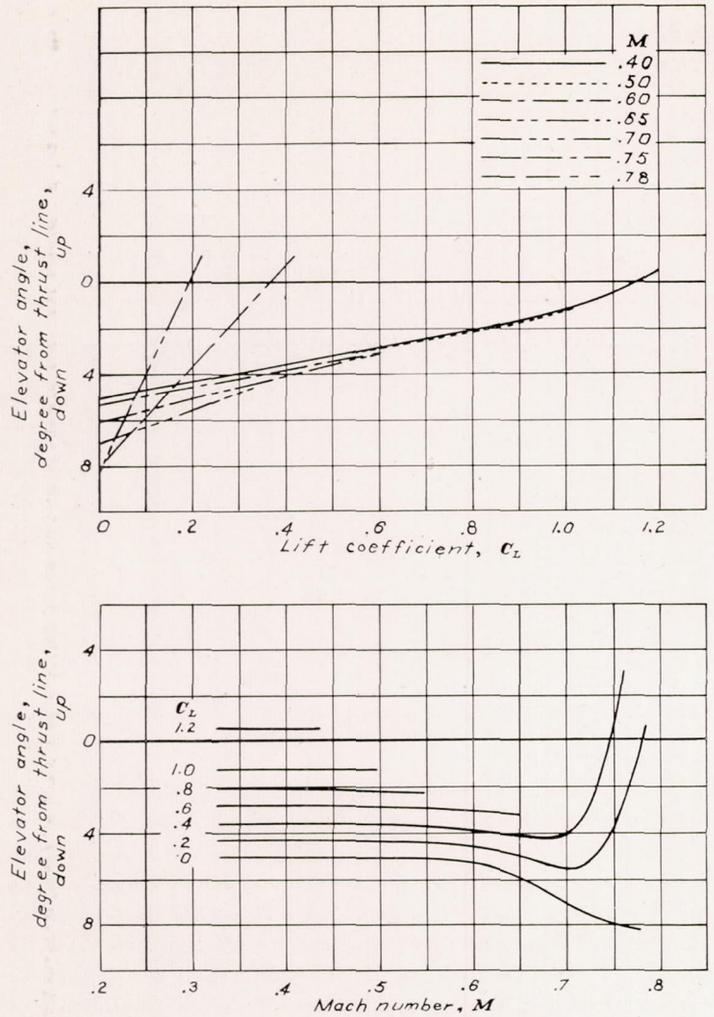

FIGURE 14.—Variation of elevator angle with lift coefficient and Mach number; clean condition, tab neutral, center of gravity at 0.288 M. A. C.

in figure 18. The elevator angle required to overcome only these moments then was computed and is compared in figure 19 with the angle measured in flight.

The remaining curves were computed from the foregoing general data. Figure 20 shows the variation with indicated airspeed of the stick force required to balance the airplane at a normal acceleration factor of 1.0 and an altitude of 15,000 feet; in addition to the forces actually measured in flight, a curve is shown calculated on the assumption that the elevator hinge-moment coefficient was not affected by bulging or compressibility, and another on the further assumption that the airplane pitching-moment coefficient was not affected by compressibility. Figure 21 shows the variation with indicated airspeed of the stick-force gradient in accelerated flight for the same conditions as those specified in figure 20. Figure 22 shows, as a function of indicated airspeed, the acceleration that would be obtained in a stick-release pull-out and in a pull-out with a 50-pound-pull stick force at an altitude of 15,000 feet.

RESULTS AND DISCUSSION

THE LOWER MACH NUMBER DATA

Stick-fixed longitudinal stability.—The curves of elevator angle and rate of change of elevator angle with lift coefficient, shown as functions of C_L and center-of-gravity position in figure 7, in general, exhibit entirely normal characteristics. It is seen that the stick-fixed neutral point in the power-off condition varied from 0.335 M. A. C. at C_L=0.12 to 0.324 M. A. C. at C_L=0.6. The neutral point in the power-on condition varied from 0.347 M. A. C. at C_L=0.12 to 0.332 M. A. C. at C_L=0.6. The fact that the neutral point with power off was ahead of that with power on probably was due, principally, to two factors:

1. The destabilizing effect of the substantially higher propeller-blade angles used in the power-off condition (fig. 6).

2. The stabilizing effect of the thrust moment in the power-on condition (constant b. h. p.) as the speed changes with C_L. (The center of gravity of the airplane lies about two-thirds foot below the thrust line and is probably very near the center of drag.)

Stick-free longitudinal stability.—The curves of stick-force modulus and rate of change of this parameter with C_L, shown as functions of C_L and center-of-gravity position in figure 8, exhibit normal characteristics in the higher test C_L range but not at the lower values of C_L. The value of the stability parameter $[d(F_e/q)/dC_L]$ is seen to become abnormally large at the lower C_L's, and the slope $\frac{d(F_e/q)/dC_L}{dx}$ actually reverses

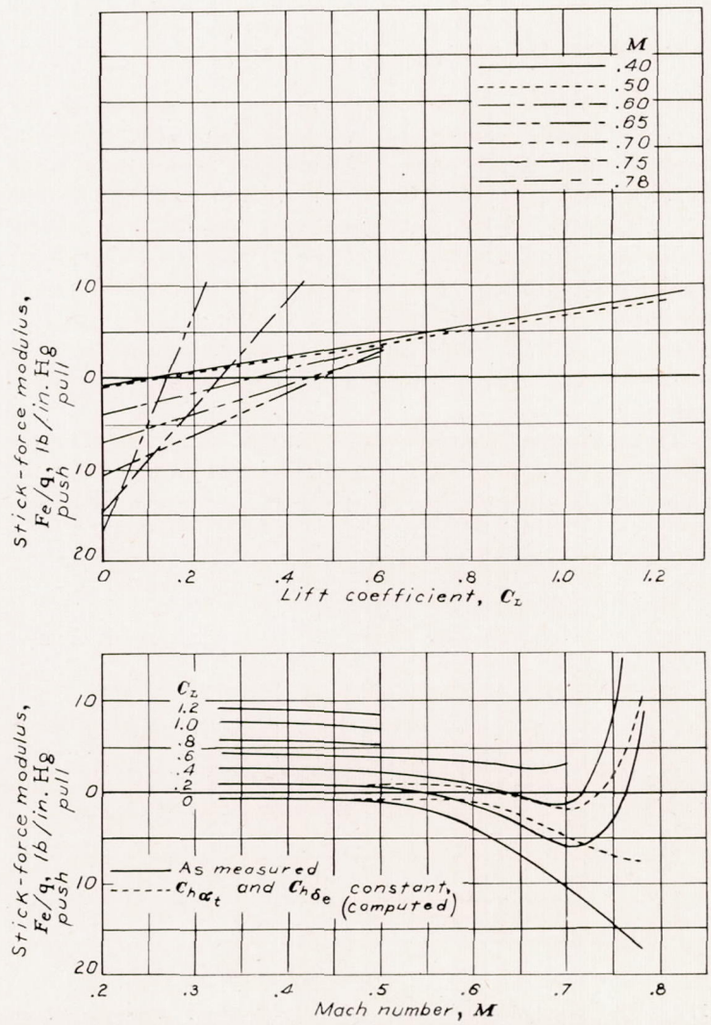

FIGURE 15.—Variation of the elevator stick-force modulus with lift coefficient and Mach number; clean condition, tab neutral, center of gravity at 0.288 M. A. C.

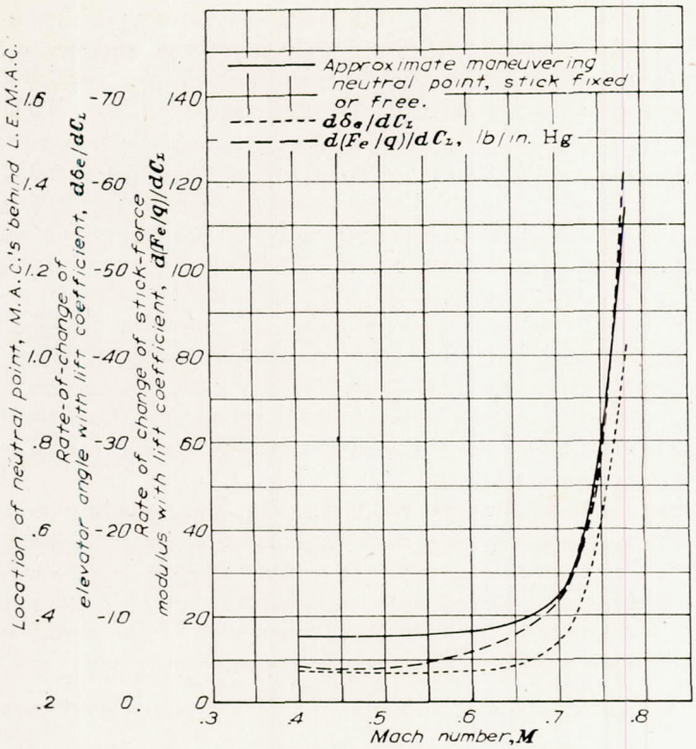

FIGURE 16.—Variation with Mach number of the stability parameters $d\delta_e/dC_L$ and $d(F_e/q)/dC_L$, and the position of the maneuvering neutral point; clean condition, tab neutral, c. g. at 0.288 M. A. C.

sign so that the stick-free stability becomes greater as the center of gravity moves back. As a result, the stick-free neutral point in the power-off condition varies from 0.348 M. A. C. at C_L=0.55 to 0.385 M. A. C. at C_L=0.25 to 0.60 M. A. C. at C_L=0.185; in the power-on condition the neutral point varies from 0.315 M. A. C. at C_L=0.55 to 0.385 M. A. C. at C_L=0.25 to 0.60 M. A. C. at C_L=0.185; and for both power conditions the neutral point moves infinitely far aft (no change in stability with center-of-gravity position) at a C_L of about 0.15, reappearing ahead of the airplane at lower values of C_L.

These peculiar characteristics cannot be ascribed to the effects of Mach number as the highest test value of this parameter was about 0.55, well under M_{cr} for the wing at low

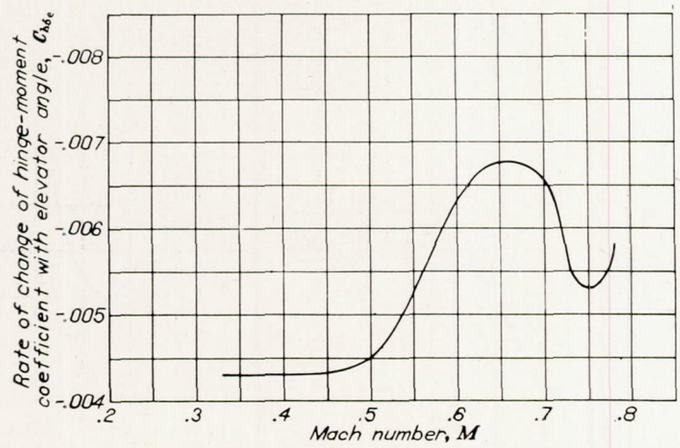

FIGURE 17.—Variation with Mach number of the rate of change of hinge-moment coefficient with elevator angle.

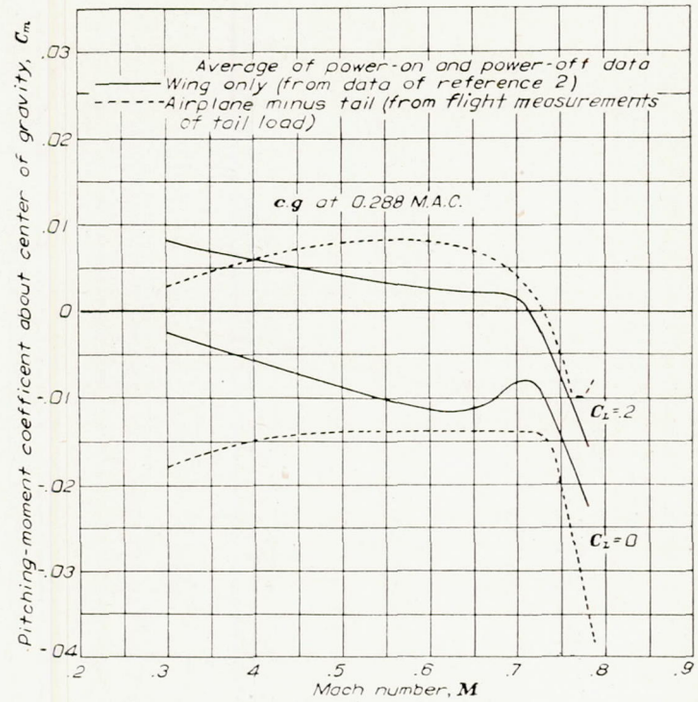

FIGURE 18.—Variation of wing pitching-moment coefficient and airplane-minus-tail pitching-moment coefficient with Mach number.

lift coefficients. The effects are, however, typical of those resulting from bulged elevator fabric when down-elevator is required to balance (as in this instance) and the internal pressure in the elevators is of the same order of magnitude as the free-stream static pressure. (See reference 3 and fig. 9.) The altered hinge-moment characteristics (as indicated by the stick forces) result from the changed profile of the control surface, which in turn depends directly on the magnitude of the pressure over it, the pressures increasing directly with dynamic pressure and elevator deflection. It is logical, then,

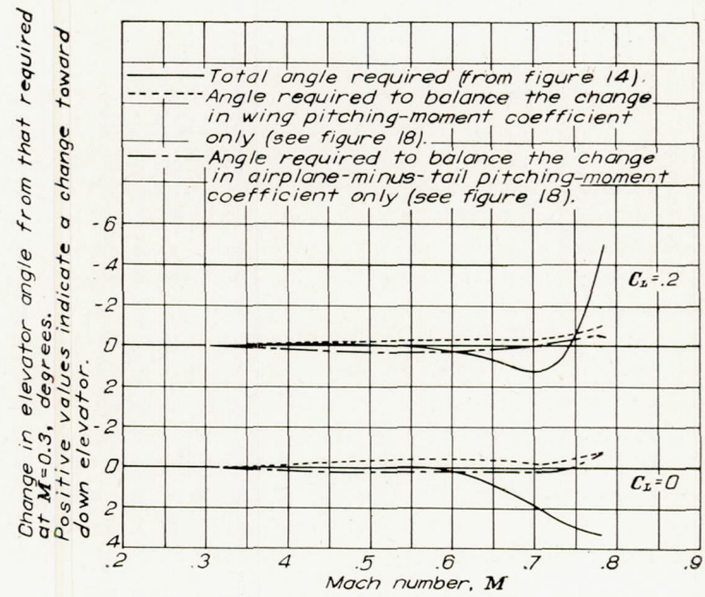

FIGURE 19.—Comparison of the change with Mach number of the actual elevator angle required, the angle necessary to balance the change in wing pitching moment only, and the angle needed to balance the change in airplane-minus-tail pitching moment only; clean condition, tab neutral, c. g. at 0.288 M. A. C.

for the effects of bulging to predominate at low lift coefficients and with the more rearward center-of-gravity locations for the following reasons:

1. In this type of test, where C_L is changed by varying the speed, the dynamic pressure and the rate of change of dynamic pressure with C_L grow rapidly large as C_L decreases. (See fig. 8.)

2. Greater down-elevator angles are required to balance the rearward shift of weight.

Profiles of a typical elevator section between ribs (fig. 10) show that the general trend is toward bulging of both the upper and lower forward surfaces of the elevator and marked cusping near the trailing edge. In addition, the maximum bulge ordinate, especially at the higher Mach numbers, is located farther aft on the top surface than on the bottom surface.[2] The source of the increased push forces required at high speeds is therefore readily apparent because the cusping of the trailing edge changes $C_{h_{\delta_e}}$ in a negative direction (reference 4), thus increasing the push forces required for a given down-elevator deflection, and the greater persistence of convexity toward the trailing edge of the upper surface produces a curvature of the mean camber line tending to produce a negative hinge moment, requiring an additional push force at the stick.

While maintenance of a high degree of stick-free stability with far rearward center-of-gravity locations allows smooth handling of an airplane in spite of the presence of stick-fixed instability, the associated elevator distortion on this airplane also produced a large change of elevator stick force required for balance as the speed increased. This detrimental effect will be discussed later in more detail.

THE HIGHER MACH NUMBER DATA

Stick-fixed longitudinal stability and control.—The variation with Mach number of the rate of change of elevator angle with lift coefficient (figs. 11, 14, and 16), indicates a stability increase starting at a Mach number of about 0.6. At a Mach number of 0.78 the stability parameter $d\delta_e/dC_L$ is −41.5, as compared with the low-speed value of −3.5.

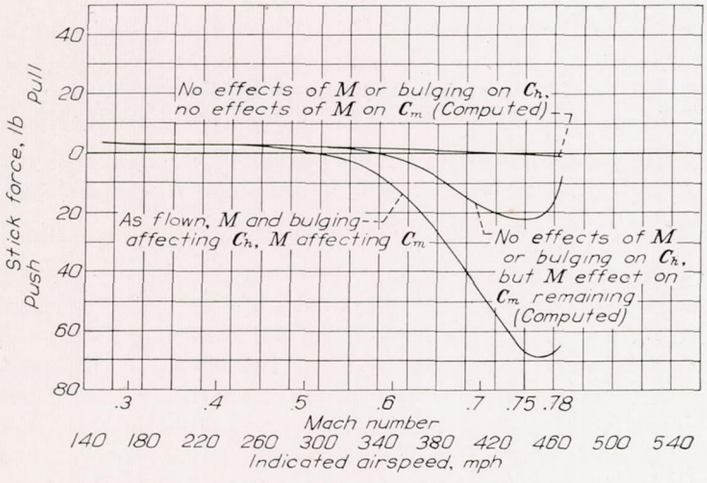

FIGURE 20.—Variation with indicated airspeed of the stick force required to balance the airplane at a normal acceleration factor of 1.0 and at an altitude of 15,000 feet; clean condition, trim tab neutral, center of gravity at 0.288 M. A. C.

[2] The elevator is vented around the hinge cut-outs and by ¼-inch diameter holes in each bay of the lower-surfaces fabric about 1½ inches from the trailing edge.

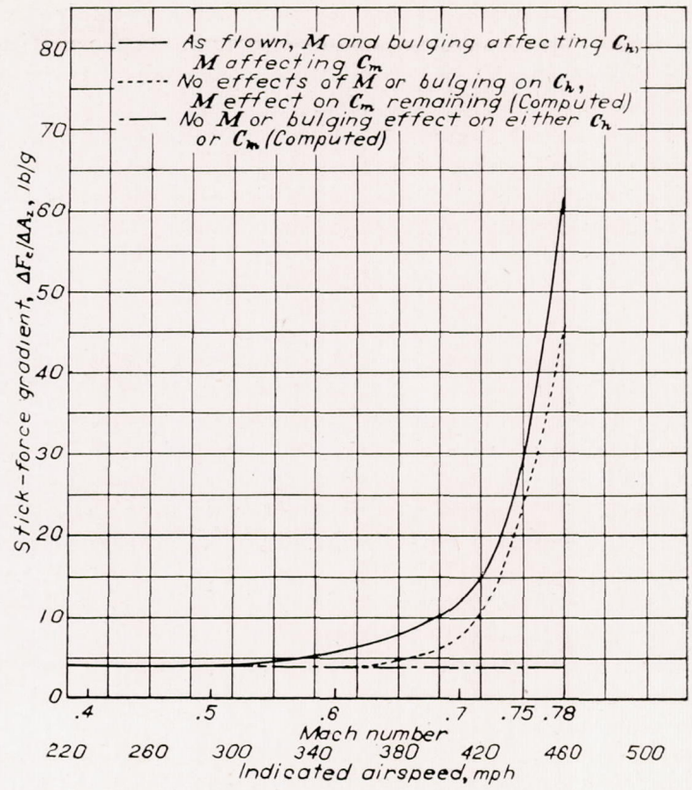

FIGURE 21.—Variation with indicated airspeed of the stick-force gradient at an altitude of 15,000 feet; clean condition, trim tab neutral, center of gravity at 0.288 M. A. C.

According to reference 5, the increase of stability at the higher Mach numbers is a characteristic trend arising from the shock-stalling of the wing and persisting until a similar stall occurs on the tail. The stability increase results principally from the increased rate of change of wing angle of attack with lift coefficient, resulting directly in a greater rate of change of tail angle of attack with airplane lift coefficient. A greater stabilizing moment is thus produced by the tail for a given change in lift coefficient and a greater change in elevator angle is required to balance the airplane.

A reduction in the ability of the elevator to change the airplane pitching moment also would result in increased values of $d\delta_e/dC_L$. Tests in the Ames 16-foot high-speed

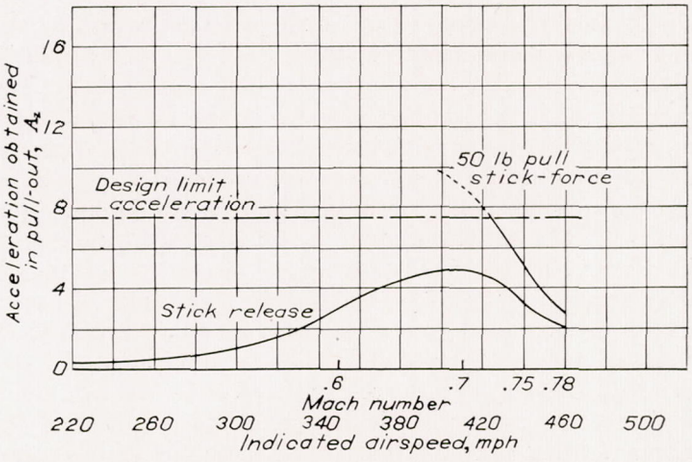

FIGURE 22.—Variation with indicated airspeed of the acceleration obtained in two types of pull-outs at an altitude of 15,000 feet; clean condition, trim tab neutral, center of gravity at 0.288 M. A. C.

wind tunnel, however, have shown essentially constant values of $dC_m/d\delta_e$ up to a Mach number of 0.80 on airplanes with tail surfaces up to 12 percent thick. The tail of the test airplane is about 8 percent thick.

It is instructive to note the shift in neutral point indicated by the foregoing data. The neutral point and its change with Mach number (fig. 16) were estimated by substituting the experimental values of $d\delta_e/dC_L$ in the following formula:

$$\frac{x'}{c}=-\frac{(d\delta_e/dC_L)a_t\tau S_t l_t}{Sc}$$

The value of a_t was adjusted for variations in Mach number by dividing the low-speed value, 0.60, by $(1-M^2)^{1/2}$. The value of τ was estimated as 0.62 and was assumed to be unaffected by compressibility. The dynamic pressure at the tail was assumed equal to the free-stream dynamic pressure. The neutral point is seen to vary from about 0.35 M. A. C. at $M=0.4$ to 0.36 M. A. C. at $M=0.6$ to 1.34 M. A. C. at $M=0.78$.

As this series of data was obtained principally in curvilinear flight, the neutral point should properly be called a maneuvering neutral point. The approximate rearward movement of the neutral point due to pitching of the airplane may be expressed as follows:

$$\Delta\frac{x'}{c}=-\frac{(-\Delta d\alpha_t/dC_L)a_t S_t l_t}{Sc}$$

An average value of $\Delta d\alpha_t/dC_L$ for this group of tests was 0.34, resulting in a value of $\Delta(x'/c)$ of about 1 percent of the M. A. C. The straight-flight neutral point at low Mach numbers was, then, at about 34 percent of the M. A. C.; this value agrees well with that determined from the static-stability tests at four center-of-gravity positions (fig. 7).

The variation with Mach number of the elevator angle required for balance at a constant lift coefficient (figs. 11, 12, and 14) indicates the gradual onset of a stick-fixed stalling-moment increment starting at a Mach number of about 0.5. At positive values of the lift coefficient, this stalling moment changes rather rapidly to a diving moment at the higher values of Mach number.

The diving moment at the higher Mach numbers, according to reference 5, and as will be shown later, results principally from the increased tail angle of attack caused by the increased airplane angle of attack required to maintain a given positive lift coefficient after the shock stall. The gradual onset of a stalling moment at the moderate Mach numbers, however, is not a general characteristic of airplanes at low lift coefficients and does not originate as a pitching moment on the wing or airplane-minus-tail group. (See fig. 18.) At positive values of the lift coefficient, the change in elevator angle (stalling-moment increment) is in the direction required to offset the change in tail angle of attack due to the increased slope of the wing lift curve in this Mach number range. The stalling-moment increment is also present, however, at a lift coefficient of zero; this fact might indicate that in this Mach number range the parts of the airplane (wing and propeller) ahead of the tail are operating at positive values of lift when the airplane lift coefficient is zero, the resulting local downwash at the tail necessitating down-elevator deflections to maintain balance. Extrapolation of some of the lift-distribution data of reference 2, for wing sections ahead of the right tail 43- and 78-percent-span stations, supports this indication; the wing section-lift coefficients are, however, too small to account for any but a small fraction of the elevator angles shown. The only major remaining possibility, then, is that the stalling moment results from a negative shift of the airplane angle of zero lift, an unusual, although possible, phenomenon.

Stick-free longitudinal stability and control.—The variation with Mach number of the rate of change of the stick-force modulus with lift coefficient (figs. 11, 15, and 16) indicates a stability increase starting at a Mach number of about 0.5. At a Mach number of 0.78 the stick-free stability parameter $d(F_e/q)/dC_L$ is 122, as compared with the low-speed value of 8.

The variation with Mach number of the stick-force modulus required for balance at constant lift coefficient (figs. 11, 13, and 15) indicates the gradual onset of a stick-free stalling moment starting at a Mach number of about 0.4 to 0.5. At appreciable values of the lift coefficient, this stalling moment changes rather rapidly to a diving moment at the higher values of Mach number.

It is seen that the stick-free characteristics of the airplane are very similar to the stick-fixed characteristics. This fact intimates that large changes in the hinge-moment parameters toward overbalance do not occur. In order to determine the magnitude of the change in stick force due to bulging and Mach number, the hinge-moment parameters $C_{h_{\alpha_t}}$ and $C_{h_{\delta_e}}$ were estimated from the data taken at Mach numbers of 0.4 and below. The negligible shift between stick-fixed and stick-free neutral points, as shown for both power conditions in figures 7 and 8, indicated that $C_{h_{\alpha_t}}$ was approximately zero. Other data (fig. 16) then indicated that $C_{h_{\delta_e}}$ was about -0.0043. Using these values, the dotted curves of figure 15 were computed, showing the values of stick-force modulus that would have been obtained if there were no effects of bulging or Mach number on the hinge-moment parameters. The principal effects of the bulging are seen to be an increase in the push forces required for balance and an increase in the value of $d(F_e/q)dC_L$ for a given Mach number. The significance of these changes will be discussed further in a later section of the report.

On the assumption that the change in $C_{h_{\alpha_t}}$ with Mach number was small enough to be negligible, the data of figure 16 were used to compute the variation of $C_{h_{\delta_e}}$ with Mach number. (See fig. 17.) The value of $C_{h_{\delta_e}}$ thus determined was found to increase from -0.0043 at $M=0.4$ to -0.0068 at $M=0.65$, and then decrease to about -0.0055 in the range $M=0.73$ to 0.78. The hook in the end of the curve shown in figure 17 may be only the result of the fairing of the cross-plotted data. The increase in the numerical value of the derivative in the first part of the curve is probably the result of the fabric bulging; at Mach numbers above 0.65 this effect apparently is overshadowed by the usual trend toward overbalance of balanced control surfaces at high Mach numbers shown by available data from high-speed wind-tunnel tests.

As a further result of the assumption that $C_{h_{\alpha_t}}$ remains

essentially zero, the stick-free neutral point will coincide with the stick-fixed neutral point in all conditions.

ADDITIONAL DERIVED DATA

Elevator angle required to balance wing pitching moment and airplane-minus-tail pitching moment.—It is interesting to determine the relative amounts of the change, with Mach number, of the elevator angle required to balance the change in the wing pitching moment alone, or the change in airplane-minus-tail pitching moment, and that required to balance the change in tail angle of attack. The change in elevator angle required to balance the change in wing pitching-moment coefficient or airplane-minus-tail pitching-moment coefficient was computed as follows:

$$\Delta\delta_e=\frac{(-\Delta C_{m_w} \text{ or } \Delta C_{m_{A-t}})Sc}{a_t\tau S_t l_t}$$

The same assumptions were made concerning the variation at a_t and τ with Mach number as had been made previously, so that

$$\Delta\delta_e=62.5(\Delta C_{m_w} \text{ or } \Delta C_{m_{A-t}})(1-M^2)^{1/2}$$

The values of ΔC_{m_w} and $\Delta C_{m_{A-t}}$ were taken from figure 18

The results (fig. 19) show that very little of the elevator-angle change was required to overcome the change in pitching moment of the wing or airplane-minus-tail group, substantiating the statement made previously that the principal changes in balance and stability at high Mach numbers were caused by the increase in tail angle of attack and in the rate of change of tail angle of attack with lift coefficient. A tailless airplane, then, might be expected to encounter less trouble from changes in stability and balance at high Mach numbers than does the conventional type.

Stick forces required to balance at various speeds.—The data so far presented (figs. 11, 13, and 15) have shown, for moderate values of lift coefficient, the usual onset of a diving moment as high Mach numbers are reached; thus diving moment is replaced by a stalling moment, however, at very low lift coefficients. The change in lift coefficient with Mach number in a straight dive is such that zero lift coefficient is approached at higher speeds, the effect of the negative change in zero-lift angle (see earlier discussion) is predominant, and a stalling moment in encountered throughout the dive. This characteristic contributes to the maintenance of push forces throughout the entire upper part of the speed range in straight diving flight.

The variation, with indicated airspeed, of the stick force required to balance the airplane in a dive at 15,000 feet (fig. 20) shows that the maximum push force required (69 pounds) exceeded the value of 50 pounds specified by reference 6, although it did not exceed the value of $(n-1)$ (Q) specified by reference 7. (For values of Q, see next section.) The pilot found the high push forces at high speeds very uncomfortable and regarded them as hazardous. It is believed, therefore, that the requirement of reference 6 is more suitable than that of reference 7.

If the effects of bulging and compressibility on the hinge-moment coefficient could have been eliminated, the maximum push force required for the same tab setting would have been only 22 pounds. The larger push force actually required was mainly the result of the elevator fabric distortion, as high Mach numbers usually tend to increase the control-surface-balance effectiveness. The advantages of limiting the elevator-contour distortion to negligible values by use of stiffer surfaces are apparent.

By considering the expression for the stick force due to a symmetrical control surface with neutral tab and $C_{h_{\alpha_t}}=0$,

$$F_e=K_e b_e \bar{c}_e^2 q C_{h_{\delta_e}} \delta_e$$

it can be seen that, in spite of the fabric distortion, the stick-force change with speed in a dive also could have been reduced by increasing the stabilizer incidence so that the elevator angle (with reference to the stabilizer) required at high speed was approximately zero.

Figure 20 also shows that the stick-force change with speed could have been still further reduced by eliminating the stick-fixed balance change with Mach number.

Stick-force-gradient variation with speed.—The variation with indicated airspeed, of the stick-force gradient at an altitude of 15,000 feet (fig. 21) shows that a value of Q of 4 pounds per g was obtained up to an indicated airspeed of 290 miles per hour; the gradient then increased, at first slowly but then more rapidly, until a value of 61.5 pounds per g was obtained at a speed of 460 miles per hour. Because of the change in stick-fixed stability, a change in Q at high speeds also would have been obtained even if the control-surface hinge-moment parameters remained constant; figure 21 shows that the increase would not have started, however, until 350 miles per hour was reached, and the value at 460 miles per hour would have been 45 pounds per g, smaller but still rather large. Elimination of the change in stick-fixed stability with Mach number, therefore, would most effectively limit the increase of Q in this instance. Lesser improvements could be obtained by limiting the change in $C_{h_{\delta_e}}$ by use of closer rib spacing, plywood, or metal surfaces. Changing the stabilizer setting would not materially alter the value of Q obtained.

The variation, with indicated airspeed, of the acceleration factor that would be obtained in two types of pull-outs (fig. 22) was computed from the data in figures 20 and 21. It is shown that, as the speed and the Mach number decrease in a near-terminal-speed pull-out with this airplane, the acceleration obtained for a given stick force increases rapidly. This type of variation admits the possibility of a pilot inadvertently overloading the airplane as a sizable pull force which at one speed produced only a moderate pull-out could, unless relaxed rapidly, result in excessive load factors as the speed decreased. A point of further interest also can be brought out here. It has become customary to warn pilots against using the trim tab to pull out of a high Mach number dive, the theory being that the tab, while relatively ineffective at the highest Mach numbers, would suddenly become effective as altitude and Mach number decreased in the dive, thus causing a sudden violent pull-out. The previous discussion suggests that, even with no change in tab setting during the pull-out, the same effect might be produced by the combined changes in trim and stability of an airplane as the Mach number decreased in the dive.

CONCLUSIONS

The following conclusions result from the data presented herein and apply specifically to the airplane, the conditions, and the range of variables tested:

1. Stick-fixed stability:

(*a*) The neutral point at low Mach numbers was at an average location of about 0.34 M. A. C.

(*b*) The stability increased markedly at Mach numbers above 0.6, and the corresponding neutral point moved well aft. At a Mach number of 0.78 the neutral point was at about 1.34 M. A. C.

(*c*) The increase in stability at high Mach numbers was found to be almost entirely the result of the increased rate of change of tail angle of attack with airplane lift coefficient.

2. Stick-fixed balance:

(*a*) At constant lift coefficient, as the Mach number was increased above about 0.5, a gradual stalling moment was introduced. This stalling moment, resulting from a negative change in the angle of zero lift and from changes in downwash at the tail, was maintained to the highest limits of the tests (M=0.78) at very low lift coefficients.

(*b*) As the Mach number increased above approximately 0.7 at moderate values of the lift coefficient, a diving moment was obtained. This moment was almost entirely the result of the increased tail angle of attack resulting from the greater airplane angle of attack necessary to maintain a given lift coefficient after the wing shock stall.

3. Stick-free stability:

(*a*) The neutral point at moderate speeds and Mach numbers was at about 0.34 M. A. C.

(*b*) As the speed increased, regardless of the Mach number, distortion of the elevator fabric occurred in such a manner as to increase the stability and move the neutral point, as determined in steady straight flight, far rearward.

(*c*) When measured in steady accelerated flight, the stick-force gradient maintained its low-speed value of 4 pounds per g to a Mach number of about 0.5, then gradually increased to 61.5 pounds per g at a Mach number of 0.78. About 70 percent of this change was caused by the increase in stick-fixed stability, the remainder being caused by the effects of fabric distortion and compressiblity on the elevator hinge moment. As nearly as could be determined, the stick-free maneuvering neutral point corresponded with the stick-fixed maneuvering neutral point.

4. Stick-free balance:

(*a*) The stick-free-balance changes with Mach number were similar in direction to the stick-fixed-balance changes although they were greatly magnified by the elevator fabric distortion.

(*b*) With the tab set to obtain zero stick force at an indicated airspeed of 300 miles per hour at 15,000 feet, the push force required near the maximum allowable speed at the same altitude was excessive (69 pounds). This force could have been reduced about two-thirds by eliminating the elevator-fabric distortion.

(*c*) The change in trim stick force with speed, when combined with the change in stick-force gradient with speed in accelerated flight, presents the possibility of inadvertently obtaining excessive loads on the airplane in a constant-stick-force pullout at high Mach number if the speed decreases rapidly.

AMES AERONAUTICAL LABORATORY,
NATIONAL ADVISORY COMMITTEE FOR AERONAUTICS,
MOFFETT FIELD, CALIF.

APPENDIX A

SYMBOLS

The symbols used throughout this report are defined below:

GENERAL

W	airplane weight, pounds.
V_i	correct indicated airspeed, miles per hour.
V	true airspeed, feet per second (except as noted).
ρ	density of the air, slugs per cubic foot.
δ_e	elevator angle, degrees (from thrust line).
α_t	tail angle of attack, degrees.
M	Mach number, ratio of V to speed of sound in free stream.
M_{cr}	critical Mach number (that Mach number at which the local speed of sound is reached at some point in the air flow over a body).
A_Z	the algebraic sum of the components along the airplane Z-axis, of the airplane acceleration and the acceleration due to gravity, in terms of g the standard gravitational unit (32.2 feet per second per second), positive when directed upward.
n	positive limit load factor, 7.5 for this airplane.
$C_{h_{\alpha_t}}$	rate of change of elevator hinge-moment coefficient with tail angle of attack at constant elevator angle $(\partial C_h/\partial \alpha_t)$.
$C_{h_{\delta_e}}$	rate of change of elevator hinge-moment coefficient with elevator angle at constant-tail angle of attack $(\partial C_h/\partial \delta_e)$.
a_t	rate of change of tail lift coefficient with tail angle of attack at constant elevator angle $(\partial C_{L_t}/\partial \alpha_t)$.
τ	elevator effectiveness $[(\partial C_{L_t}/\partial \delta_e)/\partial C_{L_t}/\partial \alpha_t)]$.
K_e	elevator control-system mechanical advantage (F_e/HM), ft^{-1}.
Q	stick-force gradient in accelerated flight (dF_e/dA_Z), lb/g.

PRESSURES

H	free-stream total pressure, pounds per square foot.
p	free-stream static pressure, pounds per square foot.
p_0	standard atmospheric pressure at sea level, pounds per square foot.
p_e	elevator internal pressure, pounds per square foot.
q	dynamic pressure $(\frac{1}{2}\rho V^2)$, pounds per square foot. (except as noted).

LENGTHS AND AREAS

x	distance parallel to the airplane X-axis, feet (positive forward).
x'	distance from *c.g.* to stick-fixed neutral point, feet.
c	length of M. A. C., feet.
$\overline{c_e}$	mean elevator chord, feet.
b_e	elevator span, feet.
l_t	distance from *c.g.* to aerodynamic center of tail, feet.
S	wing area, square feet.
S_t	horizontal tail area, square feet.

FORCES AND MOMENTS

L	lift, pounds.
L_t	tail lift, pounds.
F_e	elevator control force, pounds.
$M_{c.g.}$	pitching moment about *c.g.*, pound feet.
M_w	pitching moment of wing about *c.g.*, pound feet.
M_{A-t}	pitching moment of airplane minus tail about *c.g.*, pound feet.
HM	elevator hinge moment, pound feet.

COEFFICIENTS

C_L	lift coefficient (L/qS, or WA_Z/qS as used in this report).
C_{L_t}	tail lift coefficient (L_t/qS_t).
C_m	pitching moment coefficient $(M_{c.g.}/qSc)$.
C_{m_w}	pitching moment coefficient of wing (M_w/qSc).
$C_{m_{A-t}}$	pitching moment coefficient of airplane minus tail (M_{A-t}/qSc).
C_h	elevator hinge-moment coefficient $(HM/qb_e\overline{c_e}^2)$.
P_e	elevator internal-pressure coefficient $[(p_e-p_o)/q]$

APPENDIX B

AIRPLANE DIMENSIONS

The specifications of the airplane used in the conduct of this investigation are as follows:

Airplane, general:	
Span	34.0 feet.
Length	30.167 feet.
Height (at rest)	9.271 feet.
Wing:	
Airfoil section:	
Root (22 inches outboard of center line of airplane)	NACA 0015.
Tip (projected, 204 inches outboard of center line of airplane)	NACA 23009.
Area, total, including ailerons and section projected through fuselage	213. 22 square feet.
Chord:	
Root (22 inches outboard of center line of airplane)	8.22 feet.
Tip (projected 204 inches outboard of center line of airplane)	4.17 feet.
Mean aerodynamic chord	6.72 feet.
Dihedral, at 30 percent upper ordinate	4.0°.
Incidence, with respect to thrust line	2.0°.
Sweepback, leading edge	4.58°.
Horizontal tail:	
Span	13.00 feet.
Area	40.99 square feet.
Distance, normal gross-weight center of gravity to ⅓ maximum chord point	14.95 feet.
Elevator:	
Span	13.00 feet.
Area, total	16.89 square feet.
Balance area forward of hinge line	4.30 square feet.
Weight: Gross, normal, and approximate as flown	7,629 pounds.
Center-of-gravity position: Normal gross weight, gear up	0.285 M. A. C.
Engine:	
Type	V–1710–85.
Ratings, without ram:	

	Brake horsepower	Manifold pressure	Engine speed (r. p. m.)	Altitude (ft.)
Take-off	1, 200	51. 5	3, 000	Sea level
Military	1, 125	44. 5	3, 000	15, 500
Normal	1, 000	39. 0	2, 600	14, 000

Engine-propeller speed ratio	2.23:1.
Propeller: Type	3-blade hollow-steel selective automatic-pitch.
Blade model	A–20–156–17.
Maximum pitch limits:	
Nominal	28° to 63°.
Measured	28.7° to 65.3°.

APPENDIX C

COMPARISON WITH DATA ON SIMILAR AIRPLANE

Handling qualities of an earlier version of this airplane were measured at the lower Mach numbers at Langley Memorial Aeronautical Laboratory. The aerodynamic design of this airplane is the same as the airplane used in the tests presented in this report. Certain comparisons can be made from similar data obtained on each airplane.

NEUTRAL POINTS

The straightflight neutral-point data for the Langley test airplane for $C_L=0.2$ and 0.8 were average in the maximum level-flight speed condition and in the gliding condition for comparison with the low-speed power-on and power-off data for $C_L=0.5$ obtained in the present investigation. (See figs. 7 and 8.) The comparison is facilitated by the following table:

Airplane condition	Stick-fixed neutral point		Stick-free neutral point	
	Langley test airplane	Ames test airplane	Langley test airplane	Ames test airplane
Power on	0.33 M. A. C.	0.34	0.33	0.32
Power off	.36	.33	.35	.35

It is seen that a rearward shift of the stick-fixed neutral point with power was obtained in the present tests; while a forward shift was reported for the Langley test airplane. As discussed previously, it is believed that the rearward shift obtained in the present tests was partly the result of the shift in propeller-speed setting for the two power conditions, the higher blade angles encountered with power off (fig. 6) resulting in a greater rate of change of propeller side force with C_L in this condition. Although the propeller-speed settings used in the Langley tests are not known, it is possible that the tests were run with a fixed propeller-speed setting for both power conditions; higher blade angles would be encountered with power on than with power off, and the effect of this factor on the change in stability with power then would be opposite for the two series of tests. The agreement, however, is probably within the accuracy that neutral points can be measured.

The stick-free maneuvering neutral point in the maximum level-flight speed condition for the Langley test airplane was at 0.32 M. A. C., as compared with the average power-on and power-off location at 0.35 M. A. C. for the Ames test airplane at low Mach numbers. This discrepancy is probably not excessive considering that data at only two center-of-gravity positions were used in the Langley analysis, and a theoretical extrapolation of data taken with one center-of-gravity position was used in the present tests.

ELEVATOR HINGE-MOMENT PARAMETERS

Comparison of the stick-fixed and stick-free neutral points in the preceding table shows that $C_{h_{\alpha_t}}$ was substantially zero for the Langley test airplane as well as for the Ames test airplane. Using $C_{h_{\alpha_t}}$ as zero, the wind-up-turn data for the Langley test airplane indicated that $C_{h_{\delta_e}}$ was about -0.0040,

which value agrees well with the value of -0.0043 determined in the present tests. For the maximum level-flight-speed condition and the gliding condition, the straight-flight data for the Langley test airplane indicated that $C_{h_{\delta_e}}$ was about -0.0073, but this value may be somewhat in error as its magnitude depends directly on the slopes $\frac{d(F_e/q)/dC_L}{dx}$ and $\frac{d\delta_e/dC_L}{dx}$ determined by points at only two center-of-gravity positions. Similar data taken in the present investigation indicated a value of $C_{h_{\delta_e}}$ varying with lift coefficient; the value never became numerically greater than -0.0051, however, at speeds below the range appreciably affected by bulging or compressibility.

STICK-FORCE GRADIENT

The stick-force gradient for the Langley test airplane in accelerated flight with a center-of-gravity location at 0.288 M. A. C. was found to be 3.3 pounds per g from interpolation of the data. The value determined herein for comparable conditions on the Ames test airplane was 4.0 pounds per g. The agreement is considered good.

REFERENCES

1. Turner, Howard L., and Rathert, George A., Jr.: Pressure Lag in Tubing Used in Flight Research. NACA RB No. 5F15, 1945.
2. Clousing, Lawrence A., Turner, William N., and Rolls, L. Stewart: Measurements in Flight of the Pressure Distribution on the Right Wing of a Pursuit-Type Airplane at Several Values of Mach Number. NACA Rep. No. 859, 1945.
3. Mathews, Charles W.: An Analytical Investigation of the Effects of Elevator-Fabric Distortion on the Longitudinal Stability and Control of an Airplane. NACA ACR No. L4E30, 1944.
4. Purser, Paul E., and Gillis, Clarence L.: Preliminary Correlation of the Effects of Beveled Trailing Edges on the Hinge-Moment Characteristics of Control Surfaces. NACA CB No. 3E14, 1943.
5. Hood, Manley J., and Allen, H. Julian: The Problem of Longitudinal Stability and Control at High Speeds. NACA Rep. No. 767, 1943.
6. Anon.: Stability and Control Requirements for Airplanes. Spec. No. C–1815, U. S. Army Air Forces, Aug. 31, 1943.
7. Anon.: Stability and Control Requirements for Airplanes. Spec. No. R–1815–A, U. S. Army Air Forces, Apr. 7, 1945.

U. S. GOVERNMENT PRINTING OFFICE: 1948

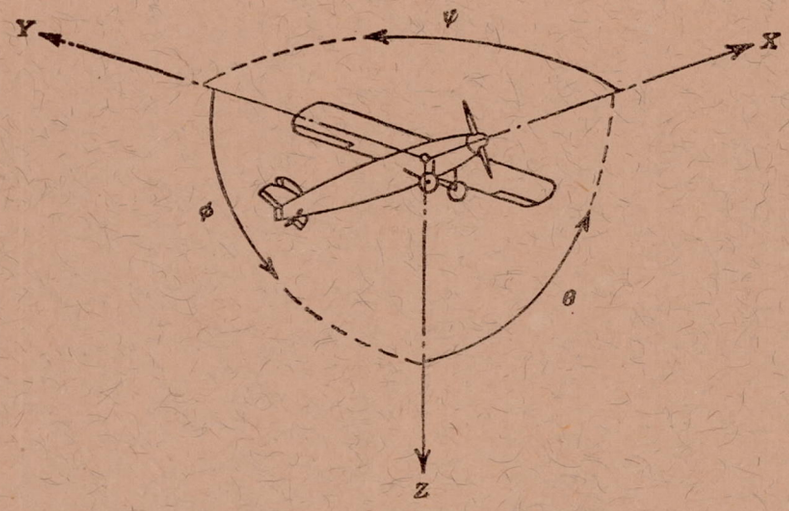

Positive directions of axes and angles (forces and moments) are shown by arrows

Axis		Force (parallel to axis) symbol	Moment about axis			Angle		Velocities	
Designation	Symbol		Designation	Symbol	Positive direction	Designation	Symbol	Linear (component along axis)	Angular
Longitudinal	X	X	Rolling	L	$Y \longrightarrow Z$	Roll	φ	u	p
Lateral	Y	Y	Pitching	M	$Z \longrightarrow X$	Pitch	θ	v	q
Normal	Z	Z	Yawing	N	$X \longrightarrow Y$	Yaw	ψ	w	r

Absolute coefficients of moment

$C_l = \frac{L}{qbS}$ (rolling) $\quad C_m = \frac{M}{qcS}$ (pitching) $\quad C_n = \frac{N}{qbS}$ (yawing)

Angle of set of control surface (relative to neutral position), δ. (Indicate surface by proper subscript.)

4. PROPELLER SYMBOLS

D Diameter

p Geometric pitch

p/D Pitch ratio

V' Inflow velocity

V_s Slipstream velocity

T Thrust, absolute coefficient $C_T = \frac{T}{\rho n^2 D^4}$

Q Torque, absolute coefficient $C_Q = \frac{Q}{\rho n^2 D^5}$

P Power, absolute coefficient $C_P = \frac{P}{\rho n^3 D^5}$

C_s Speed-power coefficient $= \sqrt[5]{\frac{\rho V^5}{P n^2}}$

η Efficiency

n Revolutions per second, rps

Φ Effective helix angle $= \tan^{-1}\left(\frac{V}{2\pi r n}\right)$

5. NUMERICAL RELATIONS

1 hp=76.04 kg-m/s=550 ft-lb/sec

1 metric horsepower=0.9863 hp

1 mph=0.4470 mps

1 mps=2.2369 mph

1 lb=0.4536 kg

1 kg=2.2046 lb

1 mi=1,609.35 m=5,280 ft

1 m=3.2808 ft